

The Chapman-type rearrangement in *pseudosaccharins*: The case of 3-(methoxy)-1,2-benzisothiazole 1,1-dioxide

A. Kaczor^{a,b,*}, L.M. Proniewicz^b, R. Almeida^{a,c}, A. Gómez-Zavaglia^{a,d}, M.L.S. Cristiano^c,
A.M. Matos Beja^e, M. Ramos Silva^e, R. Fausto^a

^a Department of Chemistry, University of Coimbra, Coimbra, 3004-535, Portugal

^b Faculty of Chemistry, Jagiellonian University, Ingardena 3, 30-060 Krakow, Poland

^c Department of Chemistry and Biochemistry, F.C.T., and CCMAR, University of Algarve, Campus de Gambelas, 8005-039 Faro, Portugal

^d Faculty of Pharmacy and Biochemistry, University of Buenos Aires, C.P. 1113 Buenos Aires, Argentina

^e Department of Physics, University of Coimbra, Coimbra 3004-536, Portugal

ARTICLE INFO

Article history:

Received 2 April 2008

Received in revised form 27 May 2008

Accepted 30 May 2008

Available online 12 June 2008

Keywords:

Pseudosaccharyl ether

Molecular structure

Reaction path

IR spectra

Matrix-isolation

DFT calculations

ABSTRACT

The thermal Chapman-type rearrangement of the *pseudosaccharin* 3-(methoxy)-1,2-benzisothiazole 1,1-dioxide (MBID) into 2-methyl-1,2-benzisothiazol-3(2*H*)-one 1,1-dioxide (MBIOD) was investigated on the basis of computational models and knowledge of the structure of the reactant and product in the isolated and solid phases. X-ray diffraction was used to obtain the structure of the substrate in the crystalline phase, providing fundamental structural data for the development of the theoretical models used to investigate the reaction mechanism in the condensed phase. The intra- and different intermolecular mechanisms were compared on energetic grounds, based on the various developed theoretical models of the rearrangement reactions. The energetic preference (ca. 3.2 kJ mol⁻¹, B3LYP/6-31+G(d,p)) of inter-over intramolecular transfer of the methyl group is predicted for the “quasi-simultaneous” transfer of the methyl groups model, explaining the potential of MBID towards [1,3′]-isomerization to MBIOD in the condensed phases. The predicted lower energy of MBIOD relative to MBID (ca. 60 kJ mol⁻¹), due to the lower steric hindrance in the MBIOD molecule, acts as a molecular motor for the observed thermal rearrangement.

© 2008 Elsevier B.V. All rights reserved.

1. Introduction

Pseudosaccharins (substituted 1,2-benzisothiazole 1,1-dioxides) have attracted attention as significant intermediates in organic synthesis, with particular emphasis on their *O*-ethers, known as important intermediates for the hydrogenolysis of alcohols. The key for the reactivity of this family of compounds is the strong electron withdrawing ability of the *pseudosaccharyl* group which reflects in its exceptionally long and short C_A–O and C_R–O bonds (where R = heteroaromatic ring and A = aliphatic or aryl group), respectively [1–3]. This characteristic structural feature of *pseudosaccharyl O*-ethers is considered to be responsible for the high ability of the *pseudosaccharyl*-oxygen system to act as nucleofuge in reductive cleavage reactions catalyzed by transition metals [1,2,4]. The ability of *pseudosaccharyl* ethers towards the cleavage of the weak C_A–O bond has also been observed in other reactions, such as the Claisen- and Chapman-like thermal isomerizations resulting in formation of *N*-isomers [3,5].

Classically, the Chapman rearrangement is assumed to be intramolecular for aryl imidates [6–8] and alkoxyprymidines [9]. On the other hand, the Chapman-type thermal rearrangement of the simplest alkyl*pseudosaccharyl* ether, 3-(methoxy)-1,2-benzisothiazole 1,1-dioxide (MBID), resulting in [1,3′]-isomerization to 2-methyl-1,2-benzisothiazol-3(2*H*)-one 1,1-dioxide (MBIOD) (Fig. 1), was observed long ago to occur in the molten phase and was suggested to take place *via* an intermolecular mechanism [10]. Recently, it was demonstrated that this process can also happen in the crystalline state [5].

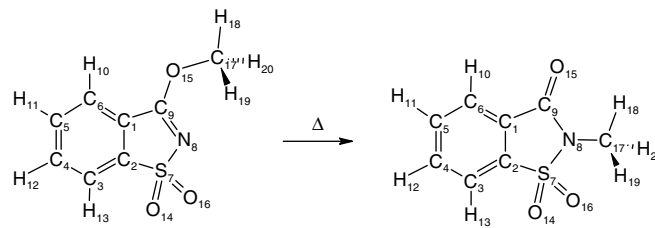


Fig. 1. The Chapman-type rearrangement of MBID (the atom numbering schemes for MBID and MBIOD adopted throughout this paper are those presented in the figure).

* Corresponding author. Address: Faculty of Chemistry, Jagiellonian University, Ingardena 3, 30-060 Krakow, Poland.

E-mail address: kaczor@chemia.uj.edu.pl (A. Kaczor).

Intermolecular Chapman-like rearrangements in the solid phase were previously described for oxadiazoles [11,12]. Intermolecular methyl migration in the solid state was also observed for methyl *p*-dimethylaminobenzenesulfonate [13–15] and 2-(4'-nitroanilino)4,6-dimethoxy-1,3,5-triazine [16]. Interestingly, for both the oxadiazoles and dimethylaminobenzenesulfonate the reaction in the solid phase was found to be faster than in the melt, and this observation was rationalized in terms of an optimal alignment of the reacting atoms in the crystal lattice of the studied compounds [11,13]. This type of rearrangements, which proceed faster in the solid than in the melt, are recognized as “topochemically controlled” and have also been previously observed for methyl group transfer reactions in thiocyanurates [17] and 4,6-dimethoxy-3-methyl-dihydro-triazine-2-one [18].

The observation that the rearrangement of MBID may take place in the solid-state [5] motivated us to shed some light on the mechanism of this reaction. To account for the intermolecularity of the observed reaction, the theoretically predicted intra- and various intermolecular reaction pathways were investigated in this study. In order to ensure applicability of the proposed models and to characterize in deeper detail the relevant chemical species, matrix-isolation infrared spectroscopy was used to obtain the vibrational spectrum of the monomeric final product (MBIOD), which was compared with previously obtained data for the monomeric substrate (MBID) [19]. The crystallographic structure of the substrate was determined through X-ray diffraction analysis.

2. Materials and methods

2.1. Experimental

MBIOD was obtained from MBID by heating a neat sample of this latter compound at *ca.* 185 °C and keeping the sample at this temperature until all reactant has been consumed, as confirmed by TLC analysis. MBIOD was isolated as colourless crystals: m.p.

Table 1
Summary of X-ray data collection and processing parameters for MBID structure

| | |
|--|---|
| Chemical formula | C ₈ H ₇ NO ₃ S |
| Colour/shape | Colourless/plate |
| Formula weight | 394.43/2 |
| Space group | P1 |
| Temperature, K | 293(2) |
| Cell volume (Å ³) | 430.08(10) |
| Crystal system | Triclinic |
| <i>a</i> (Å) | 6.9412(9) |
| <i>b</i> (Å) | 7.7281(10) |
| <i>c</i> (Å) | 8.1558(11) |
| α (deg) | 100.044(7) |
| β (deg) | 92.511(7) |
| γ (deg) | 91.670(7) |
| Formula units/unit cell | 2 |
| <i>D_c</i> (Mg m ⁻³) | 1.523 |
| Diffractometer/scan | APEX II KAPPA CCD/ ω , ϕ |
| Radiation (Å) (graph. monochromated) | 0.71073 |
| Max crystal dimensions (mm) | 0.26 × 0.16 × 0.06 |
| θ Range (deg) | 2.54–28.34 |
| Range of <i>h, k, l</i> | –9/9, –10/10, –10/10 |
| Reflections measured/independent | 17231/2117 (<i>R</i> _{int} = 0.0221) |
| Reflections observed <i>I</i> > 2 σ | 1779 |
| Corrections applied | Lorentz and polarization effects |
| Computer programs | SHELXL, SHELXS, PLATON |
| Structure solution | Direct methods |
| No. of parameters varied | 119 |
| GOF | 1.062 |
| <i>R</i> 1 | 0.0322 |
| <i>wR</i> 2 | 0.0865 |
| Function minimized | $\Sigma w(\Delta F^2)^2$ |
| Diff. density final max/min (e Å ⁻³) | 0.278/–0.312 |

129–130 (C; 1H NMR (300 MHz, CDCl₃), 3.28 (3H, s), 7.80–7.90 (2H, m), 7.92–7.96 (1H, d), 8.05–8.10 (1H, d); MS (EI): *m/z* 197 ([M]⁺, 100%). The synthesis of MBID was described elsewhere [5,19].

The infrared spectra were recorded in the 500–4000 cm⁻¹ range using a Mattson Infinity 60AR series FT-IR spectrometer, with resolution of 0.5 cm⁻¹. The sample was co-deposited with xenon (N45, Air Liquide) isolant gas onto a cryogenically cooled (20 K) CsI window. The compound was sublimated at *ca.* 340 K from a specially designed mini-furnace assembled inside the cryostat. The selected temperature of the CsI optical substrate was obtained using an APD Cryogenics closed-cycle helium refrigeration system with a DE-202A expander. The temperature was measured directly at the sample holder by a silicon diode temperature sensor, connected to a digital controller (Scientific Instruments, Model 9650-1) with the accuracy of 0.1 K. Detailed descriptions of experimental conditions applied to obtain spectra of matrix-isolated MBID as well as polycrystalline spectra of both compounds may be found elsewhere [5,19].

X-ray data were collected on a Bruker APEX II-CCD diffractometer, using a transparent plate shaped crystal with dimensions 0.26 × 0.16 × 0.06 mm. The crystallographic structure was solved by direct methods using SHELXS-97 [20]. Refinements were carried out with the SHELXL-97 package [20]. All refinements were made by full-matrix least-squares on *F*² with anisotropic displacement parameters for all non-hydrogen atoms (Table 1 for details).

2.2. Computational

Geometry optimizations and calculations of vibrational frequencies of MBIOD were performed at the DFT/B3LYP level of theory [21,22], using the 6-31+G(d,p), 6-31++G(3df,3pd) and 6-311++G(3df,3pd) basis sets.

The intrinsic reaction coordinate (IRC) reaction path for the intramolecular rearrangement of MBID into MBIOD was calculated at the B3LYP/6-31++G(3df,3pd) level of theory and the geometry and other relevant properties of the transition state (TS) associated to this process were obtained at the same level of theory with the help of the synchronous transit-guided quasi-Newton method (STQN-QST3) [23,24]. In order to compare these results with the investigated intermolecular models, the geometry and vibrational frequencies of the substrate, product and TS state were recomputed at the B3LYP/6-31+G(d,p) level [giving energy values in close agreement with those obtained at the higher B3LYP/6-31++G(3df,3pd) level].

Three alternative reaction pathways modeling the intermolecular rearrangement were computed at the B3LYP/6-31+G(d,p) level of theory. In *model 1*, a sequential process was considered: the bond distance between the nitrogen atom of one molecule and the methyl carbon atom of the second molecule (C₁₇...N₈) was varied stepwise and all other parameters optimized at each point, producing an anion–cation pair; subsequently, a second methyl group transfer for anion–cation and neutral–anion pathways was considered by scanning the C₁₇...N₈ distance, leading to the final products (“sequential” model). In *model 2*, both C₁₇...N₈ and C₁₇...N₈ distances were varied simultaneously and the two methyl groups transferred synchronously (“simultaneous” transfer model). Finally, in *model 3*, the C₁₇...N₈ distance was varied up to *ca.* 1.9 Å, then fixed at this value while the C₁₇...N₈ distance was varied up to full first methyl group transfer and, finally, the C₁₇...N₈ distance further shortened to allow for the second methyl transfer (“quasi-simultaneous” transfer model). In all considered models, the reactant and all neutral products were fully optimized and their vibrational frequencies subsequently computed at the B3LYP/6-31+G(d,p). Further description on these models is given in the *Models for the MBID → MBIOD rearrangement* section.

All the above-mentioned calculations were performed using the GAUSSIAN 03 suite of programs [25]. Potential energy distributions (PEDs) of the normal modes were computed in terms of natural internal coordinates [26] with the GAR2PED program [27].

3. Results and discussion

3.1. Geometry of MBID: comparison between X-ray (crystal) and theoretical (isolated monomer) data

The structure of the isolated molecule of MBID was recently studied in great detail using different theoretical models [19]. In the present investigation its structure in the crystalline state has been addressed using X-ray diffraction. The X-ray crystal structure of MBID is presented in Figs. 2 and 3. Atomic coordinates, bond lengths, valence angles, dihedral angles, and other crystallographic data were deposited at the Cambridge Crystallographic Data Center CCDC No. CCDC 674704.

Apart from O₁₄ and O₁₆, in the crystal the molecules of MBID are mainly planar, with O₁₅ and C₁₇ sharing the plane of the two fused rings (Fig. 2). The O₁₄ and O₁₆ atoms are not equally far-away from such plane. The distance between O₁₆ and the least-squares plane of the rings is 1.1869(12) Å while for O₁₄ the distance is 1.2613(12) Å. The torsion angle N₈–C₉–O₁₅–C₁₇ is 1.1(2)°. There are no conventional hydrogen bonds between the molecules due to the lack of donors. Even the weaker C–H... π interactions are not observed in this structure. The closest intermolecular contact for O₁₄ is with C₁₇ⁱ (*i*: $-x, 1-y, 1-z$) at a distance of 3.319(2) Å while for O₁₆ the closest intermolecular contact is with C₆ⁱⁱ (*ii*: $1-x, -y, -z$) [3.443(2) Å]. The main interaction governing the packing of the molecules is π ... π interaction between the π electron clouds of neighboring saccharin derivatives. This interaction displays the usual slipped stacking geometry, with the interacting π systems antiparallel displaced. The centroid–centroid distance between consecutive centroids of the six-membered rings is 3.9097(9) Å and the distance between consecutive centroid of five-membered rings/centroid of six-membered rings is 3.9097(9) Å. The π ... π interactions join the molecules in columns that run along the *a* axis (Fig. 3).

The comparison between the geometrical parameters of the isolated monomer of MBID, obtained at the B3LYP/6-311++G(3df,3pd) level of theory [5], and those determined for the molecule in the crystal (Table 2), reveals the excellent correlation between the two sets of data, providing further evidence on the absence of specific strong intermolecular interactions in the crystal. Nevertheless, in the gas phase the molecule is predicted to be strictly C_s, while in

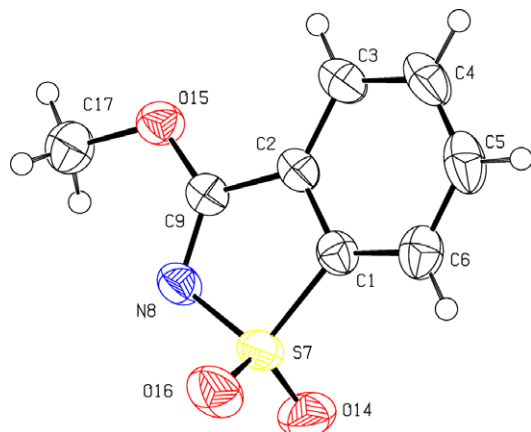


Fig. 2. ORTEP diagram of MBID, showing the displacement ellipsoids drawn at the 50% probability level.

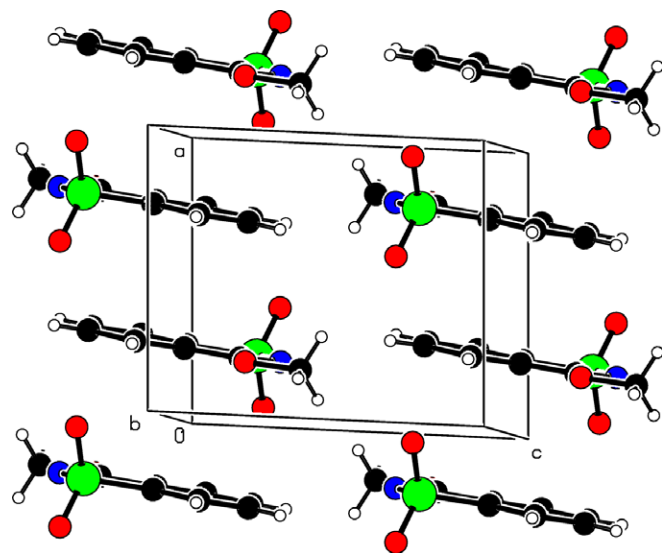


Fig. 3. Crystal packing of MBID.

the crystal it appears slightly distorted, as described above. The similarity between the gas phase and crystal state MBID molecular geometries supports the use of isolated molecule based theoretical models to address the reactivity of this molecule in the condensed phases.

3.2. Geometry of MBIOD. Comparison of the substrate and the product

There is only one minimum on the potential energy surface for MBIOD. The stable conformer of MBIOD has C_s symmetry and one of the hydrogen atoms of the methyl group in the *anti*-periplanar arrangement relatively to the S–N bond. The optimized B3LYP/6-311++G(3df,3pd) geometrical parameters of MBIOD are given in Table 2.

MBIOD was found to be significantly more stable (*ca.* 58–60 kJ mol⁻¹ depending on the level of theory applied) than MBID [19]. This difference in stability might be rationalized in terms of differences between the geometries of the two compounds. Obviously, the tautomerization reaction must affect considerably the length of the C₉–O₁₅ bond.

Although an extremely short C₉–O₁₅ bond is a characteristic feature of the *O*-ethers of *pseudosaccharins* [1–3], as mentioned in the *Introduction*, the conversion of the ether linkage (in MBID) into a carbonyl bond (in MBIOD) further shortens this bond, from 1.320 to 1.209 Å [B3LYP/6-311++G(3df,3pd) results]. This value is even smaller than that normally associated with the C–O bond length in a carbonyl of a ketone or aldehyde (1.23 Å). This change constrains considerable redistribution of the electronic density within the five-membered heterocyclic ring. The striking difference could be easily anticipated to take place in the length of the C₉–N bond, which increases from 1.284 Å in MBID to 1.386 Å in MBIOD. The changes in the lengths of the remaining bonds of the isothiazole ring nearly cancel each other, with the C–S bond being shortened by 0.023 Å and the N–S and C₂–C₉ bonds being lengthened by 0.012 and 0.010 Å, respectively. On the whole, the heterocyclic ring is predicted to be more strained in MBID than in MBIOD, with the sum of bond lengths being 0.100 Å smaller in the first molecule, while the sum of the ring-internal angles is nearly equal for both compounds. The higher steric hindrance of MBID compared with that of MBIOD is then one of the main factors responsible for the higher stability of the latter compound. It is also worth noting that the changes in the geometry of the five-membered ring upon MBID → MBIOD conversion practically do not

Table 2

Chosen experimental (X-ray; single crystal) and calculated geometrical parameters for MBID and calculated geometrical parameters for MBIOD

| Parameter | MBID | | MBIOD |
|--|-----------|-------------------------------------|--|
| | X-ray | DFT/B3LYP/ 6-311++G(3df,3pd) [5] | DFT/B3LYP/ 6-311++G(3df,3pd) |
| Bond length (Å) | | | |
| C ₁ –S ₇ | 1.767(1) | 1.791 | 1.768 |
| C ₂ –C ₉ | 1.480(2) | 1.479 | 1.489 |
| S ₇ –N ₈ | 1.653(1) | 1.679 | 1.691 |
| S ₇ =O ₁₄ | 1.431(1) | 1.434 | 1.435 |
| S ₇ =O ₁₆ | 1.430(1) | 1.434 | 1.435 |
| C ₉ =N ₈ | 1.292(2) | 1.284 | 1.386 |
| C ₉ –O ₁₅ | 1.309(2) | 1.320 | 1.209 (C ₉ =O ₁₅) |
| C ₁₇ –O ₁₅ | 1.454(2) | 1.442 | – |
| Angle (°) | | | |
| C ₂ –C ₁ –S ₇ | 106.9(1) | 107.5 | 110.2 |
| C ₆ –C ₁ –S ₇ | 130.3(1) | 130.4 | 127.3 |
| C ₁ –C ₂ –C ₉ | 109.5(1) | 109.4 | 113.4 |
| C ₃ –C ₂ –C ₉ | 129.7(1) | 130.0 | 126.5 |
| C ₁ –S ₇ –N ₈ | 96.5(1) | 94.9 | 92.0 |
| C ₁ –S ₇ –O ₁₄ | 111.3(1) | 110.4 | 111.8 |
| C ₁ –S ₇ –O ₁₆ | 111.3(1) | 110.4 | 111.8 |
| N ₈ –S ₇ –O ₁₄ | 109.1(1) | 109.3 | 109.6 |
| N ₈ –S ₇ –O ₁₆ | 108.8(1) | 109.3 | 109.6 |
| O ₁₄ =S ₇ =O ₁₆ | 117.8(1) | 119.7 | 118.7 |
| C ₉ =N ₈ –S ₇ | 109.1(1) | 109.9 | 115.4 |
| C ₂ –C ₉ =N ₈ | 118.0(1) | 118.4 | 108.9 |
| C ₂ –C ₉ –O ₁₅ | 117.4(1) | 117.6 | 126.5 |
| N ₈ =C ₉ –O ₁₅ | 124.6(1) | 124.0 | N ₈ C ₉ =O ₁₅ : 124.7 |
| C ₉ –O ₁₅ –C ₁₇ | 116.9(1) | 117.0 | C ₉ –N ₈ –C ₁₇ : 123.9 |
| O ₁₅ –C ₁₇ –H ₁₈ | 109.5 | 105.3 | N ₈ –C ₁₇ –H ₁₈ : 106.9 |
| O ₁₅ –C ₁₇ –H ₁₉ | 109.5 | 110.0 | N ₈ –C ₁₇ –H ₁₉ : 110.5 |
| O ₁₅ –C ₁₇ –H ₂₀ | 109.5 | 110.0 | N ₈ –C ₁₇ –H ₂₀ : 110.5 |
| Dihedral angle (°) | | | |
| C ₃ –C ₂ –C ₁ –S ₇ | 179.9(1) | 180.0 | 180.0 |
| C ₉ –C ₂ –C ₁ –S ₇ | 1.3(1) | 0.0 | 0.0 |
| S ₇ –C ₁ –C ₆ –H ₁₃ | 0.8 | 0.0 | 0.0 |
| C ₂ –C ₁ –S ₇ –N ₈ | –2.0(1) | 0.0 | 0.0 |
| C ₂ –C ₁ –S ₇ –O ₁₄ | 111.5(1) | 112.7 | 112.1 |
| C ₂ –C ₁ –S ₇ –O ₁₆ | –115.0(1) | –112.7 | –112.1 |
| C ₆ –C ₁ –S ₇ –N ₈ | 177.1(1) | 180.0 | 180.0 |
| C ₆ –C ₁ –S ₇ –O ₁₄ | –69.5(2) | –67.3 | –67.9 |
| C ₆ –C ₁ –S ₇ –O ₁₆ | 64.0(2) | 67.3 | 67.9 |
| C ₁ –C ₂ –C ₉ =N ₈ | 0.2(2) | 0.0 | 0.0 |
| C ₁ –C ₂ –C ₉ –O ₁₅ | 179.5(1) | 180.0 | 180.0 |
| C ₃ –C ₂ –C ₉ =N ₈ | –178.3(1) | 180.0 | 180.0 |
| C ₃ –C ₂ –C ₉ –O ₁₅ | 1.0(2) | 0.0 | 0.0 |
| C ₁ –S ₇ –N ₈ =C ₉ | 2.1(1) | 0.0 | 0.0 |
| C ₉ =N ₈ –S ₇ –O ₁₄ | –113.1 | –113.7 | –114.0 |
| C ₉ =N ₈ –S ₇ –O ₁₆ | 117.2(1) | 113.7 | 114.0 |
| C ₂ –C ₉ =N ₈ –S ₇ | –1.6(2) | 0.0 | 0.0 |
| S ₇ –N ₈ =C ₉ –O ₁₅ | 179.1(1) | 180.0 | 180.0 |
| C ₂ –C ₉ –O ₁₅ –C ₁₇ | –178.3(1) | 180.0 | C ₂ C ₉ N ₈ C ₁₇ : 180.0 |
| N ₈ =C ₉ –O ₁₅ –C ₁₇ | 1.1(2) | 0.0 | – |

influence the geometry of the six-membered ring. Indeed, the HOMA aromaticity index [28] of the phenyl ring in MBID and MBIOD (0.992 and 0.995, respectively) are practically identical and also very close to that of benzene (1.000).

3.3. Models for the MBID → MBIOD rearrangement

As it was previously suggested by Hettler [10], the Chapman-like rearrangement of MBID takes place intermolecularly [5]. An intermolecular methyl migration in the crystalline state is facilitated if a propitious arrangement of the substrate molecules in the crystal occurs, as was previously demonstrated in the case of oxadiazoles [11,12] and methyl *p*-dimethylaminobenzenesulfonate [13–15]. Under these conditions, the intermolecular methyl transfer does not require a considerable distortion of the molecules in the crystal and may become energetically favored. Nevertheless, the intermolecular methyl transfer in the solid state might also

take place if the reaction is not topochemically controlled. An interesting example of such methyl conversion is the rearrangement of 2-(4'-nitroanilino) 4,6-dimethoxy-1,3,5-triazine into a mixture of products, which occurs in the solid state although there are no contacts between the reaction centers of the substrate in the crystal [16].

In order to understand the energetic factors controlling the observed MBID → MBIOD rearrangement, models for the intra- and intermolecular processes shall be considered and compared.

The knowledge about the structures of the monomeric substrate and product discussed above, also rationalized by the good agreement between the theoretically predicted infrared spectra of the two compounds and the corresponding matrix-isolation spectra (see Fig. 4 and Table 3 for MBIOD, and Ref. [19] for equivalent spectroscopic data for MBID), together with the X-ray data obtained for the substrate, provides the basis for the development of reliable theoretical models for the MBID → MBIOD rearrangement.

Fig. 5 presents the calculated IRC reaction path [B3LYP/6-31++G(3df,3pd)], with the optimized geometries of both minima and the transition state for the intramolecular MBID → MBIOD rearrangement model.

In the transition state, the four-membered C–O–C–N ring is significantly distorted, with very long C₁₇–O and C₁₇–N distances (2.162 and 2.222 Å, respectively) and short C₉–O and C₉–N bonds (1.253 and 1.321 Å). The B3LYP/6-31++G(3df,3pd) computed energy for the TS is 287.2 and 230.6 kJ mol^{–1} higher than those for the product and reactant, respectively, showing that the predicted activation energy for the (concerted) intramolecular rearrangement is quite high (230.6 kJ mol^{–1}). The reconsideration of the reaction at the B3LYP/6-31+G(d,p) level of theory, used in the computationally more exigent intermolecular models discussed below, brought similar values, namely an activation energy of 229.2 kJ mol^{–1} and an energy difference between MBID and MBIOD equal to 58.1 kJ mol^{–1}.

The input geometry used to calculate the intermolecular rearrangement pathways was taken from the X-ray data (Fig. 6a). Two MBID molecules from neighboring layers of the crystal were chosen (Fig. 6b) to form the initial dimeric unit used in the calculations.

In the first intermolecular model investigated, the rearrangement can be considered as a sequential process in which the first step is the transfer of the methyl group from one MBID molecule to the nitrogen atom of the second molecule, giving rise to an anion–cation pair. The initial formation of an anion–cation pair was previously suggested by Dessolin et al. [11] as the initial step of oxadiazoles rearrangement, leading to propagation of the reaction via the methyl transfer between a neutral molecule and an anion or a cation. A two-step mechanism involving a molecular pair intermediate was also proposed for intermolecular thermal isomerisation of methyl *p*-dimethylaminobenzenesulfonate into zwitterionic *p*-trimethylammoniumbenzenesulfonate [15].

In our calculations we considered two pathways for the second methyl transfer: anion–cation (starting from the point in the PES corresponding to the minimum energy structure after the first methyl group transfer) and anion–neutral molecule.

In the crystal, there are two “types of pairs” of MBID molecules (see Fig. 6), with different C₁₇...N₈ distances (ca. 4 and 5 Å, respectively). In the calculations, during the initial step of the sequential intermolecular rearrangement, the C₁₇...N₈ distance (Δ_1) was decreased in steps of 0.1 Å, starting from a value equal to the longest distance of this structural parameter observed in the MBID crystal, 5.0 Å, while all other structural parameters were let to relax. During the initial steps (up to a value for the C₁₇...N₈ distance equal ca. 3.6 Å, see Fig. 7) of the transfer, the energy of the system is predicted to fluctuate only slightly, the maximal change of energy

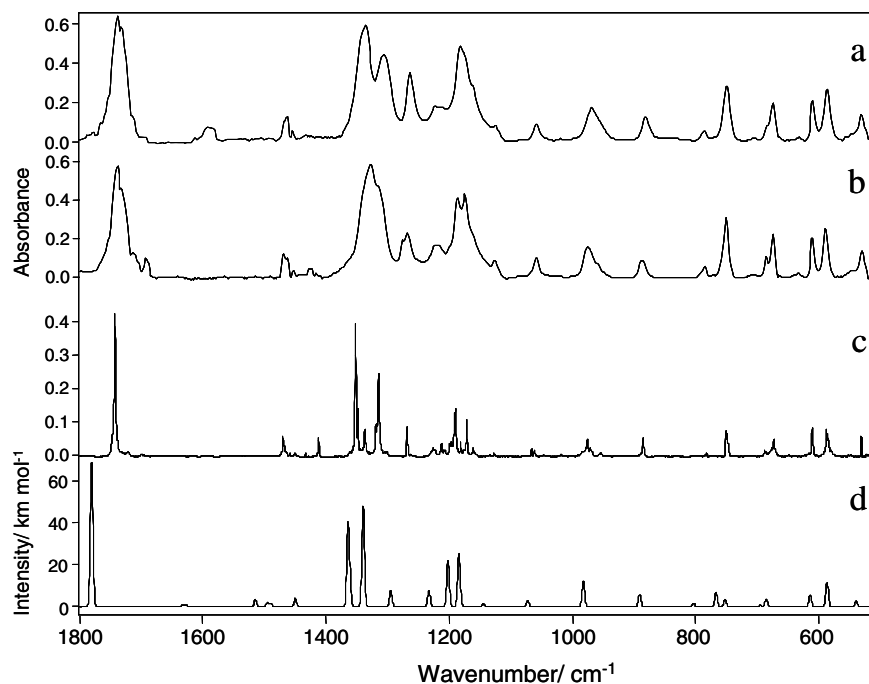


Fig. 4. Infrared spectra of MBIOD: (a) in the molten phase at 210 °C, (b) in the polycrystalline phase after cooling the melt to 20 °C, (c) isolated in the Xe matrix (20 K) and (d) B3LYP/6-311+G(3df,3pd) calculated spectrum for the monomer.

being no more than 1.6 kJ mol⁻¹. As this initial shortening of the distance does not significantly affect the energy of the system, it is suggested that up to some point the molecules in the pair behave as practically non-interacting.

Along the methyl transfer, the C₁₇...N₈ (Δ_2) distance shortens down from 5.0 Å to approximately 3.6 Å while Δ_1 reduces to 3.9 Å and, from there, it is quite conserved (fluctuating in the range 3.6–3.5 Å) until Δ_1 becomes ca. 2.1 Å. Then, a further shortening of Δ_2 occurred (down to 3.245 Å) when the methyl group was transferred and Δ_1 becomes 1.437 Å. During the initial steps of methyl transfer the model structure started to flatten but after the transition state was reached ($\Delta_1 = 1.889$ Å; see Fig. 6c) the two molecular units got significantly distorted out-of-plane relatively to each other.

The energy profile corresponding to the above described single methyl transfer process is given in Fig. 7. An activation energy of ca. 174 kJ mol⁻¹ with respect to the reactants' minimum (the fully optimized MBID dimer, where both C–N distances are equal to 3.689 Å, see Fig. 7) was obtained. Comparison with the activation energy of the methyl intramolecular transfer (229.2 kJ mol⁻¹) shows that this first step in the sequential intermolecular model is favorable on energy grounds. However, as mentioned above, in this sequential model, the first methyl group transfer corresponds only to an introductory step for the reaction and requires the subsequent transfer of a second methyl group in order to obtain the final neutral MBIOD product.

Two different pathways for the second methyl group transfer were investigated: anion–cation (starting from the point in the PES corresponding to the minimum energy structure after the first methyl group transfer) and anion–neutral molecule. The obtained energy profiles for these two pathways are presented in Fig. 8.

Both considered reaction pathways for the transfer of the second methyl group are predicted to require quite high energy. The activation energy for the anion–cation methyl transfer is ca. 175 kJ mol⁻¹, i.e. the energy of the transition state stays ca. 253 kJ mol⁻¹ above that of the initial reactant (MBID dimer; see also Fig. 7). In this transition state, the anion–cation pair shows a

significant deviation from planarity, with the N₈...C₁₇...O₁₅...C₉ dihedral and N₈...C₁₇...O₁₅ bond angles being 6.5° and 84.5°, respectively. The product is a structure in which two MBIOD molecules are arranged one on the top of the other (see Fig. 8). In turn, the activation energy for the anion–neutral molecule methyl transfer process is even higher (ca. 314 kJ mol⁻¹).

As a whole, the sequential model for intermolecular transfer of the methyl group, both for the anion–cation and anion–neutral molecule second step, is predicted to have an activation energy much higher than that corresponding to the intramolecular rearrangement. These results clearly demonstrate that the reaction cannot occur this way.

The second intermolecular model investigated assumes that simultaneous one-step transfer of two methyl groups takes place. This mechanism could be expected to be favored if proper alignment of molecules in the crystal occurred. This type of mechanisms was suggested for the solid state methyl transfer of 6-methoxy-3,5-dimethyl-tetrahydrotriazine-2,4-dione, based on the crystal structure for this compound obtained by X-ray diffraction analysis [18,29–32]. In the case of MBID, the activation energy for the simultaneous methyl transfer process was predicted to be ca. 286 kJ mol⁻¹ [B3LYP/6-31+G(d,p)] (see Fig. 7), i.e. ca. 55 kJ mol⁻¹ higher than that estimated for the intramolecular process. In fact, the MBID molecules in the crystal lattice are not favorably oriented to allow for the simultaneous methyl transfer to take place efficiently, since interaction between molecules from two different layers separated by a large distance (ca. 5 Å) would be required. In addition, steric hindrance due to repulsive interactions between the two methyl groups being simultaneously transferred (both of them placed in-between the two rearranging MBID molecules; see Fig. 7) also contributes to make this process disfavored. In consonance with this, the MBID → MBIOD rearrangement does not show the characteristics of a typical topochemically assisted reaction. The reaction in the solid state is slower than in the liquid and is considerably accelerated by melting [5].

The third model investigated (“quasi-simultaneous” model) resulted from a preliminary exploration of the potential energy sur-

Table 3Assignment of experimental IR spectra of matrix-isolated (solid Xe, 20 K), polycrystalline and melted MBIOD in KBr pellet (500–4000 cm⁻¹ spectral range)

| Calculated ^a B3LYP/6-311++G(3df,3pd) | | Experimental | | | | | | Approximate assignment ^b |
|---|-----------------------------|---------------------------|-----------|---------------------------|-------|---------------------------|-------|--|
| | | Xe, 20 K | | Polycrystalline | | Melt | | |
| ν (cm ⁻¹) | I (km mol ⁻¹) | ν (cm ⁻¹) | I^c | ν (cm ⁻¹) | I^c | ν (cm ⁻¹) | I^c | |
| 3169 | 5.4 | n.obs | – | 3095 | m | 3095 | w | $\nu\text{C-H}_{6R}$ |
| 3166 | 0.4 | n.obs | – | 3084 | sh | 3084 | w | $\nu\text{C-H}_{6R}$ |
| 3154 | 3.5 | n.obs | – | 3072 | w | 3074 | w | $\nu\text{C-H}_{6R}$ |
| 3141 | 1.5 | n.obs | – | 3035 | w | 3030 | w | $\nu\text{C-H}_{6R}$ |
| 3106 | 0.1 | 2977 | w | 3016 | w | | | $\nu\text{C-H}_M$ |
| 3073 | 7.1 | 2943 | w | 2952 | w | 2950 | w | $\nu\text{C-H}_M$ |
| 3008 | 28.6 | 2905 | w | 2925 | w | 2925 | sh | $\nu\text{C-H}_M$ |
| 1757 | 367.4 | 1742 | S | 1739 | S | 1737 | S | $\nu\text{C=O}$ |
| 1612 | 5.1 | n.obs ^d | – | 1595 | w | 1593 | w | $\nu\text{C-C}_{6R}$ |
| 1606 | 5.3 | n.obs ^d | – | | | | | $\nu\text{C-C}_{6R}$ |
| 1494 | 18.0 | 1469/1467 | m/sh | 1469 | m | 1464 | m | δ_M |
| 1477 | 6.6 | 1463 | sh | 1460 | m | 1456 | sh | $\delta\text{C-C-H}_{6R}$ |
| 1474 | 6.7 | 1458 | w | | | | | δ_M |
| 1469 | 8.3 | 1450 | w | | | | | $\delta\text{C-C-H}_{6R}$ |
| 1431 | 21.2 | 1411 | m | 1422 | m | 1422/1417 | w/sh | δ_M |
| 1346 | 208.0 | 1352/1351/1348 | S/S/m | 1328 | S | 1337 | S | $\nu\text{S=O}$ |
| 1343 | 28.4 | 1343/1336 | w/m | | | | | $\nu\text{C-C}_{6R}$ |
| 1322 | 257.2 | 1319/1314/1312 | m/S/sh | 1315 | S | 1308 | S | $\nu\text{C}_9\text{-N}$, $\nu\text{C}_{17}\text{-N}$ |
| 1278 | 41.5 | 1268 | m | 1276 | m | 1264 | m | $\delta\text{C-C-H}_{6R}$ |
| 1217 | 41.5 | 1225/1222/1212/1208/1206 | w/w/m/w/w | 1221/1214 | m/sh | 1223/1213 | m/sh | δ_M , $\nu\text{C-C}_{5R}$ |
| 1186 | 118.7 | 1199/1197/1190/1192 | m/m/S/S | 1187 | S | 1183 | S | $\nu\text{S=O}$ |
| 1172 | 5.4 | 1181 | m | 1174/1160 | S/sh | 1176/1162 | sh/sh | $\delta\text{C-C-H}_{6R}$ |
| 1169 | 131.8 | 1176/1171 | sh/S | | | | | $\nu\text{S=O}$ |
| 1142 | 0.6 | 1161/1159 | w/w | 1132 | sh | 1137 | sh | δ_M |
| 1129 | 7.3 | 1127 | w | 1127 | w | 1125 | w | $\delta\text{C-C-H}_{6R}$, $\nu\text{C-C}_{6R}$ |
| 1058 | 15.7 | 1066/1061 | w/w | 1057 | m | 1059 | m | $\delta\text{C-C-C}_{6R}$ |
| 1028 | 0.8 | 1018 | w | 1022 | w | 1019 | w | $\nu\text{C-C}_{6R}$ |
| 1009 | 0.0 | n.obs | – | 999 | w | 999 | w | γ_{6R} |
| 976 | 0.6 | 984/978 | w/sh | 978 | m | 971 | m | γ_{6R} |
| 970 | 65.7 | 976/975/971/969 | m/sh/m/sh | 968 | sh | 960 | sh | $\nu\text{C}_{17}\text{-N}$, $\nu\text{C}_9\text{-N}$ |
| 896 | 0.1 | n.obs | – | n.obs | – | n.obs | – | γ_{6R} |
| 879 | 31.4 | 885 | m | 890 | m | 882 | m | $\nu\text{N-S}$, δ_M , $\delta\text{X-C=O}$ |
| 793 | 9.5 | 786/784/782 | w/w/w | 785 | w | 787 | w | $\gamma\text{C-C(=O)-N}$, γ_{6R} |
| 757 | 36.3 | 751/750/749/748 | m/m/m/m | 751 | S | 749 | S | τ_{6R} , γ_{6R} |
| 743 | 18.6 | 747 | sh | | | | | $\delta\text{C-C-C}_{6R}$ |
| 686 | 4.3 | 688/685 | w/w | 685 | m | 685 | w | $\delta\text{C-C-C}_{6R}$ |
| 676 | 20.8 | 676/673 | w/m | 675 | m | 675 | m | τ_{6R} |
| 606 | 31.5 | 611/610 | m/sh | 609 | m | 610 | m | $\delta\text{X-S=O}$, $\delta\text{X-C=O}$ |
| 579 | 62.7 | 588/586 | m/m | 591 | S | 587 | S | $\gamma\text{C-S(=O)-N}$ |
| 533 | 14.8 | 531 | m | 528 | m | 532 | m | $\gamma\text{C-S(=O)-N}$, τ_{6R} |
| 505 | 25.6 | 510 | m | 512 | m | 508 | m | $\delta\text{C-X-X}_{5R}$ |

^a Frequencies scaled uniformly by the factor of 0.987 [15].^b 6R and 5R refer to the six- and five-membered ring, respectively; M stands for methyl group; ν , δ , γ and τ indicate stretching, bending, rocking and torsion modes, respectively; X designates either a C, S or N atom.^c Experimental intensities are provided as qualitative: S, strong; m, medium; w, weak; sh, shoulder.^d Not identified probably due to overlap with the bands assigned to monomeric water.

face of the system in aiming to find the minimum reaction pathway for the intermolecular transfer. This preliminary inspection of the PES was carried out at a low-level of theory [B3LYP/3-21G(d,p)], since it required the calculation of a two-dimensional energy grid resulting from the PES scan along the Δ_1 and Δ_2 coordinates. This scan was performed by varying the C...N distances in the 2.8–1.8 Å range, in steps of 0.1 Å; see Fig. 9.

The results of this preliminary PES study confirm that the most energetically favorable methyl transfer pathway is indeed along the C...N coordinates, with Δ_1 first varying down to 1.8 Å and then Δ_2 being shortened while Δ_1 is kept at that value.

Following the indications provided by the preliminary examination of the PES along the C...N coordinates, calculations performed at the B3LYP/6-31+G(d,p) level of theory were carried out: starting with the geometry extracted from the X-ray data, the Δ_1 distance was initially changed down to 1.889 Å and from this point the shortening of the Δ_2 distance was conducted while Δ_1 was kept frozen; when the Δ_2 distance reduces to 1.5 Å, the Δ_1 distance was then shortened down to 1.449 Å while Δ_2 was allowed to relax (Fig. 10).

The activation energy for this “quasi-simultaneous” methyl transfer process is *ca.* 226 kJ mol⁻¹, in respect to the fully optimized substrate. The predicted energy is then considerably lower than the energy of all other considered intermolecular pathways of rearrangement and slightly lower (*ca.* 3.2 kJ mol⁻¹) than the activation energy of the intramolecular transfer. The significant energetic preference of the “quasi-simultaneous” mechanism of rearrangement over the other intermolecular mechanisms results from the fact that in its transition state a more favorable equilibrium is attained between the two most relevant factors determining the activation barrier: the value of the N₈...C₁₇...O₁₅ angle (a more linear angle favors energetically the process) and the steric repulsion between the methyl groups. As described before, the first factor favors the simultaneous transfer of the methyl groups (for this mechanism the N₈...C₁₇...O₁₅ angle at the transition state is *ca.* 166°), but the second factor was highly unfavorable. In turn, the repulsion between the methyl groups is minimized in the sequential mechanism, which however is disfavored by the strong deviation from linearity of the N₈...C₁₇...O₁₅ angle (*ca.* 85°). On the other hand, for the *quasi-simultaneous* mechanism, the

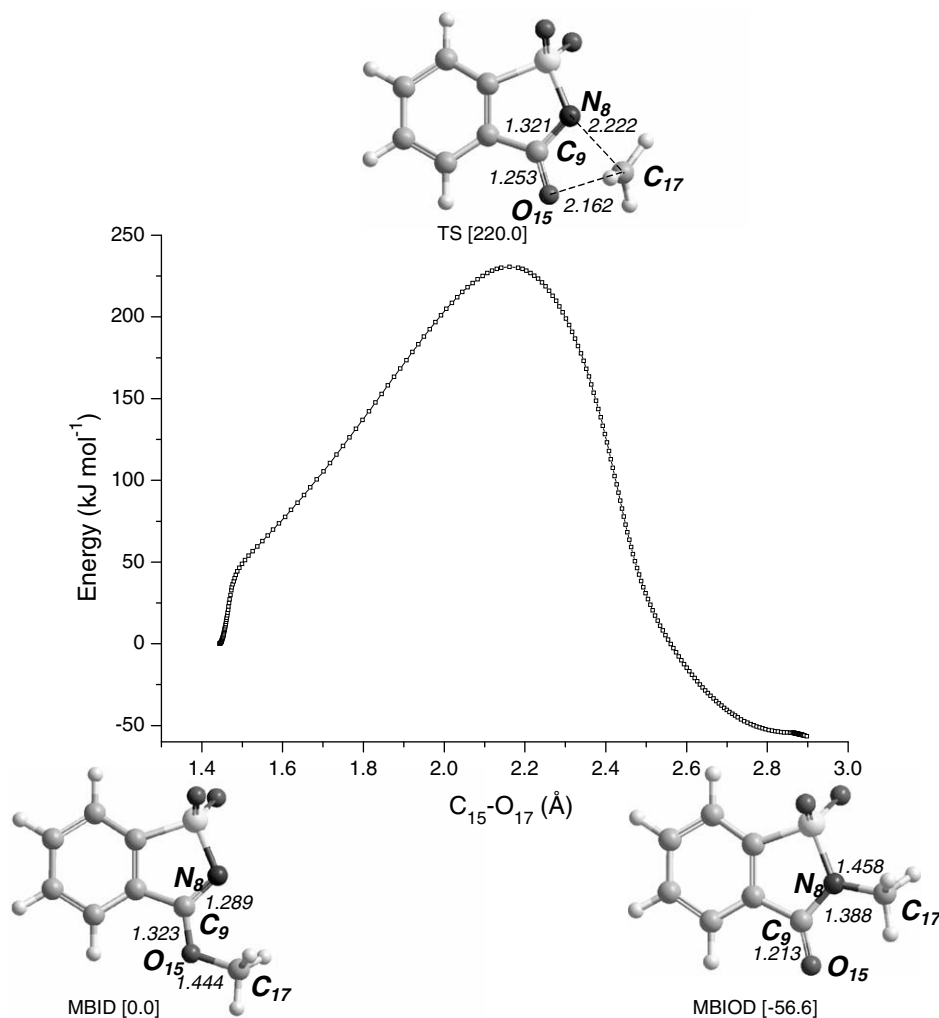


Fig. 5. The predicted IRC reaction path [B3LYP/6-31++G(3df,3pd)] for the intramolecular rearrangement of MBID to MBIOD. Optimized geometries for the substrate, product and the TS are shown, with the key bond lengths presented explicitly. The zero-point corrected energies relative to the substrate (in kJ mol⁻¹) are given in brackets. The numbering of the relevant atoms is shown (bold).

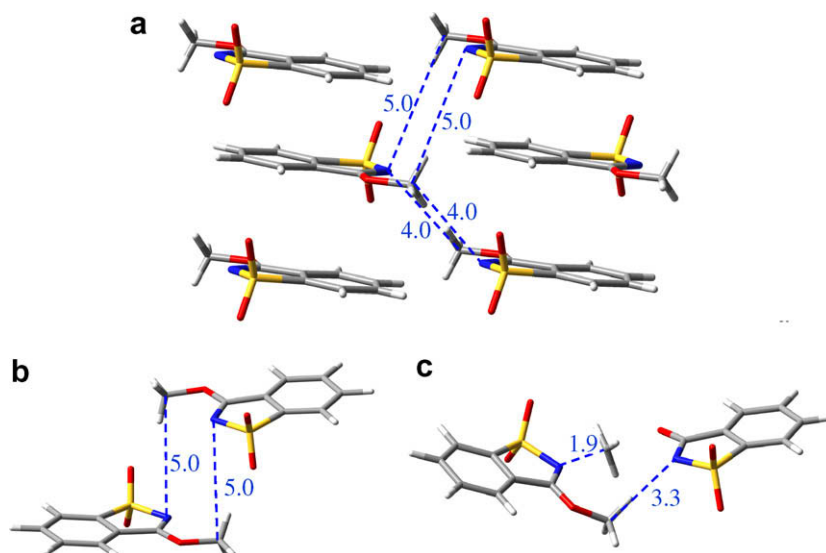


Fig. 6. (a) MBID pair arrangements in the crystal, (b) the input structure used in the theoretical intermolecular rearrangement models and (c) the geometry of the model at the transition state after flattening of the structure.

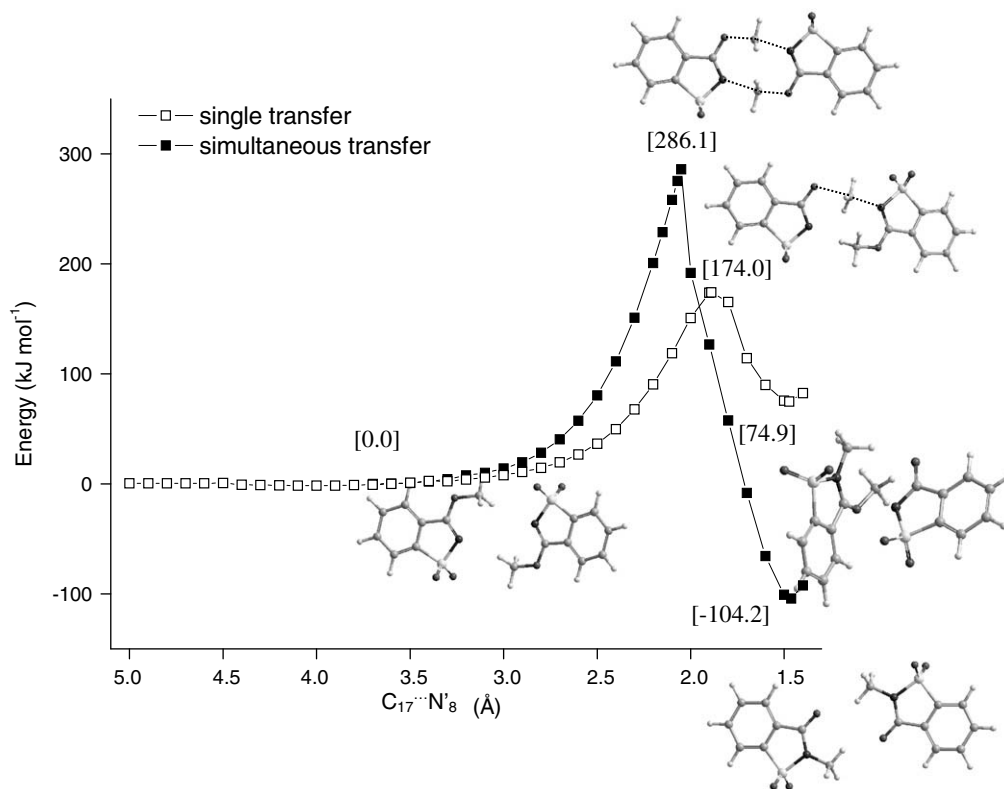


Fig. 7. Calculated reaction paths [B3LYP/6-31+G(d,p)] for the intermolecular rearrangement of MBID to MBIOD: (□) the first methyl group transfer in the sequential model; (■) the simultaneous transfer of two methyl groups. Relative energies (in kJ mol^{-1}) of reactant, product and transition state species are given in brackets.

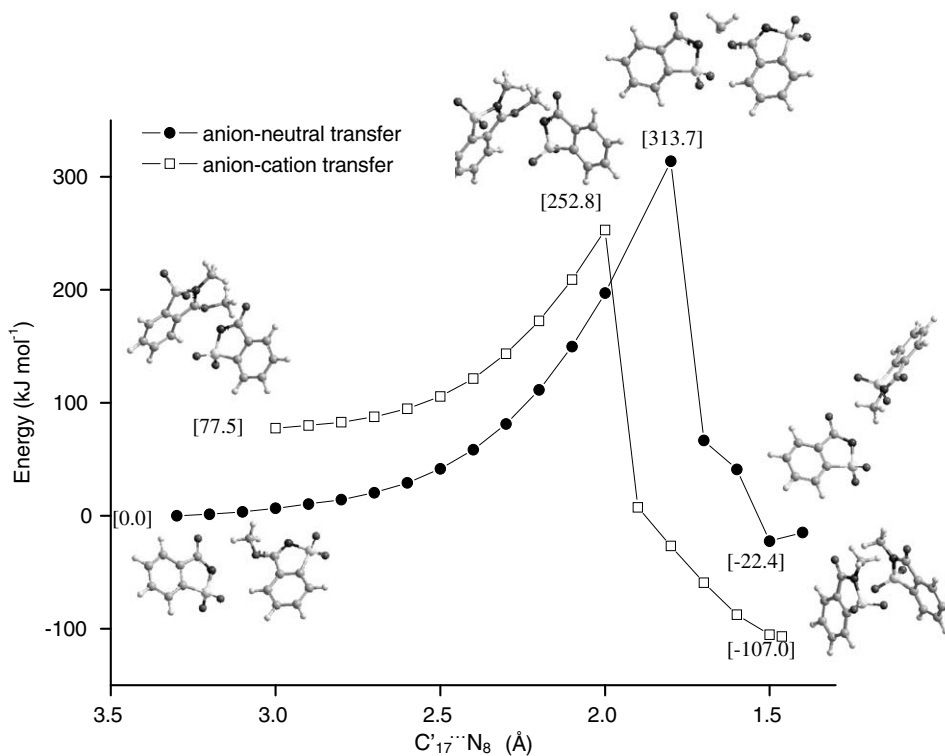


Fig. 8. Calculated reaction paths [B3LYP/6-31+G(d,p)] for the second step of the sequential intermolecular rearrangement of MBID into MBIOD: (□) via anion-cation; (●) via anion-neutral molecule (●). The energies (kJ mol^{-1}) relative to the fully optimized substrate (for anion-cation reaction) and to the starting structure (for the anion-neutral reaction) are given in brackets.

$\text{N}_8 \cdots \text{C}'_{17} \cdots \text{O}'_{15}$ angle is *ca.* 130° in the transition state and the repulsive interactions between the methyl groups are also relatively

weak, since in this case the hydrogen atoms are directed in opposition to each other, conversely to what happens in the case of the

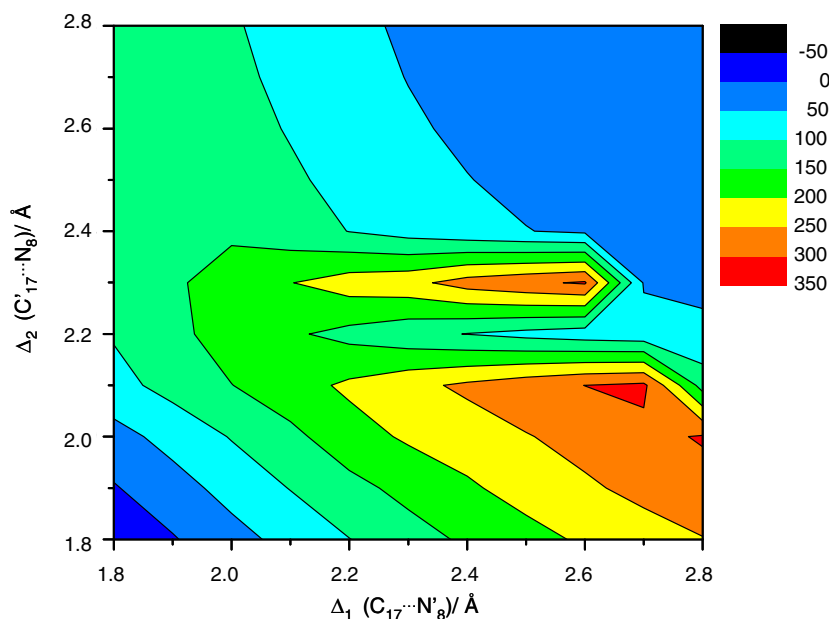


Fig. 9. Two-dimensional potential energy profile for MBID → MBIOD rearrangement (energy in kJ mol^{-1}).

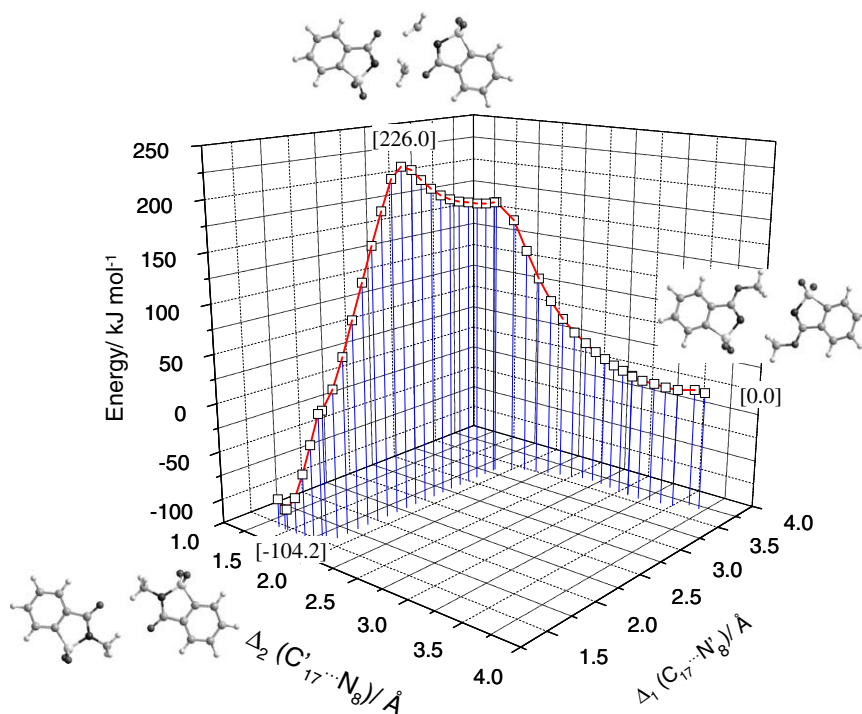


Fig. 10. The predicted reaction path [B3LYP/6-31+G(d,p)] for the “quasi-simultaneous” intermolecular methyl transfer (MBID → MBIOD). The energies relative to the fully optimized substrate are given in brackets.

simultaneous transfer, where the methyl groups are in close proximity and interact repulsively *via* four hydrogen atoms; compare Figs. 7 and 10).

Compared to the activation energy associated to intramolecular transfer, the activation energy of the “quasi-simultaneous” intermolecular process is only slightly lower (*ca.* 3.2 kJ mol^{-1}), although an upmost bending of the $\text{O}_{15}\cdots\text{C}_9\cdots\text{N}_{17}$ angle (60.8°) is predicted for the transition state of the intramolecular rearrangement. However, the intramolecular process is the only one in which the transition state is not sterically crowded. The conjugated effects of

these two factors (unfavorable deviation from linearity of the $\text{O}_{15}\cdots\text{C}_9\cdots\text{N}_{17}$ angle and favorable lack of hindrance in the TS of the intramolecular process) result in the comparable activation energy of the intra- and “quasi-simultaneous” intermolecular rearrangements.

We believe that MBID is a boundary case, for which the preference towards an inter- over intramolecular process exists. It is expected that the steric hindrance due to a substituent bigger than the methyl group would significantly increase the energy of the transition state (see Fig. 10), thus making the intermolecular rear-

rangement improbable on energetic grounds (as was noticed before, the classical Chapman rearrangement is assumed to be intramolecular for aryl imidates) [6–8]. The reaction is not topochemically controlled, therefore, it is expected that a prerequisite for the transfer is a slight reorganization of the molecules in the lattice with the shortening of both C–N distances (see Fig. 7), allowing the subsequent “quasi-simultaneous” transfer of the methyl groups. The computations suggest that the initial process of molecular reorganization does not require significant energy. However, the rigidity of the lattice, not taken into account in our dimeric-type models, shall definitely hinder in some amount this “pre-orientation” required to start the process, thus being a decisive factor in explaining the observed greater facility of MBID to undergo the rearrangement after melting [5], when the molecular mobility strongly increases and a proper alignment of the substrate molecules may be more easily attained.

4. Conclusions

The mechanism for the thermal Chapman-type rearrangement of MBID towards its energetically lower (*ca.* 60 kJ mol⁻¹) tautomer, MBIOD, was investigated in detail. Based on the knowledge of the structure of the substrate and product under different experimental conditions, various models for the rearrangement reaction were evaluated through quantum chemical theoretical methods.

Comparison of the predicted energetics for the various studied models indicates that among the intermolecular rearrangements investigated only that involving the “quasi-simultaneous” transfer of two methyl groups is energetically favored relatively to the intramolecular migration model. Both the sequential and simultaneous mechanisms for methyl transfer were found to require considerably more energy to take place (27 and 80 kJ mol⁻¹ for anionic and anion–neutral molecule sequential mechanism, respectively, and 60 kJ mol⁻¹ for the simultaneous process).

According to the “quasi-simultaneous” mechanism, the transfer of the second methyl group starts when the first methyl group is not yet fully transferred (when the C–N distance equals *ca.* 1.9 Å), the activation energy of the process being *ca.* 226 kJ mol⁻¹, slightly below to that corresponding to the intramolecular rearrangement. Two factors were found to be fundamental in controlling the energy of the methyl group transfer process: the deviation from linearity of the N₈...C₁₇...O₁₅ angle and the steric hindrance in the transition state structure. The “quasi-simultaneous” intermolecular methyl transfer was found to be the unique mechanism in which these two factors are well balanced (*e.g.*, the simultaneous methyl transfer mechanism and the intramolecular mechanism are very much disfavored by the first factor, while the sequential mechanism is strongly destabilized by the second one). The observed reaction is not topochemically controlled due to long distance in the crystal (*ca.* 5 Å) between the nitrogen and carbon atoms directly involved in the rearrangement. Therefore, the pre-orientation of the molecules in the lattice is necessary in order to allow for the methyl group transfer to take place. Although the computations predict that this process is not energetically expensive *per se*, the rigidity of the crystalline lattice, not taken into account in our dimeric-type models, shall hinder to some extent this “pre-orientation” required to start the process, thus being a decisive factor in explaining the observed greater facility of MBID to undergo the rearrangement after melting [5], when the molecular

mobility strongly increases and a proper alignment of the substrate molecules may be more easily attained.

Acknowledgements

Calculations were done at the Academic Computer Center “Cyfronet”, Krakow, Poland (Grant KBN/SGL_ORIGIN_2000/UJ/044/1999), which is acknowledged for computing time. The research was supported by the Portuguese Fundação para a Ciência e a Tecnologia (Grant FCT #SFRH/BPD/26590/2006 and Projects POCl/QUI/59019/2004, POCl/QUI/58937/2004 and PTDC/QUI/67674/2006). AGZ is member of the research career Conicet (National Research Council, Argentina). Authors wish to acknowledge Dr. Marcin Andrzejak for the helpful ideas contributing to this work.

References

- [1] N.C.P. Araújo, A.F. Brigas, M.L.S. Cristiano, L.M.T. Frija, E.M.O. Guimarães, R.M.S. Loureiro, *J. Mol. Catal. A Chem.* 215 (2004) 113.
- [2] L.M.T. Frija, M.L.S. Cristiano, E.M.O. Guimarães, N.C. Martins, R.M.S. Loureiro, J.F. Bickley, *J. Mol. Catal. A Chem.* 242 (2005) 241.
- [3] N.C.P. Araújo, P.M.M. Barroca, J.F. Bickley, A.F. Brigas, M.L.S. Cristiano, R.A.W. Johnstone, R.M.S. Loureiro, P.C.A. Pena, *J. Chem. Soc., Perkin Trans. 1* (2002) 1213.
- [4] A.F. Brigas, R.A.W. Johnstone, *Tetrahedron Lett.* 31 (1990) 5789.
- [5] R. Almeida, A. Gómez-Zavaglia, A. Kaczor, M.L.S. Cristiano, M.E.S. Eusébio, T.M.R. Maria, R. Fausto, *Tetrahedron* 64 (2008) 3296.
- [6] H.M. Rells, *J. Org. Chem.* 33 (1968) 2245.
- [7] O.H. Wheeler, F. Roman, O. Rosado, *J. Org. Chem.* 34 (1969) 966.
- [8] K.B. Wiberg, B.L. Rowland, *J. Am. Chem. Soc.* 77 (1955) 2205.
- [9] D.J. Brown, R.V. Foster, *J. Chem. Soc.* (1965) 4911.
- [10] H. Hettler, *Tetrahedron Lett.* 15 (1968) 1793.
- [11] M. Dessolin, O. Eisenstein, M. Golfier, T. Prangé, P. Sautet, *J. Chem. Soc., Chem. Commun.* (1992) 132.
- [12] M. Dessolin, M. Golfier, *J. Chem. Soc., Chem. Commun.* (1986) 38.
- [13] C.N. Sukenik, J.A.P. Bonapace, N.S. Mandel, P.-Y. Lau, G. Wodo, R.G. Bergman, *J. Am. Chem. Soc.* 99 (1977) 851.
- [14] J.A.R.P. Sarma, J.D. Dunitz, *Acta Crystallogr. B* 46 (1990) 780.
- [15] A. Gavezzotti, M. Simonetta, *Nouv. J. Chim.* 2 (1977) 69.
- [16] H. Taycher, M. Botoshansky, V. Shteiman, M. Kaftory, *Supramol. Chem.* 13 (2001) 181.
- [17] M. Greenberg, V. Shteiman, M. Kaftory, *Acta Crystallogr. B Struct. Sci.* 57 (2001) 428.
- [18] E. Handelsman-Benory, M. Botoshansky, M. Greenberg, V. Shteiman, M. Kaftory, *Tetrahedron* 56 (2000) 6887.
- [19] A. Kaczor, R. Almeida, A. Gómez-Zavaglia, M.L.S. Cristiano, R. Fausto, *J. Mol. Struct.* 876 (2008) 77.
- [20] G.M. Sheldrick, *Acta Crystallogr. A* 64 (2008) 112.
- [21] A.D. Becke, *Phys. Rev. A* 38 (1988) 3098.
- [22] C.T. Lee, W.T. Yang, R.G. Parr, *Phys. Rev. B* 37 (1988) 785.
- [23] C.Y. Peng, P.Y. Ayala, H.B. Schlegel, M.J. Frisch, *J. Comput. Chem.* 17 (1996) 49.
- [24] C.Y. Peng, H.B. Schlegel, *Isr. J. Chem.* 33 (1993) 449.
- [25] M.J. Frisch, G.W. Trucks, H.B. Schlegel, G.E. Scuseria, M.A. Robb, J.R. Cheeseman, J.A. Montgomery Jr., T. Vreven, K.N. Kudin, J.C. Burant, J.M. Millam, S.S. Iyengar, J. Tomasi, V. Barone, B. Mennucci, M. Cossi, G. Scalmani, N. Rega, G.A. Petersson, H. Nakatsuji, M. Hada, M. Ehara, K. Toyota, R. Fukuda, J. Hasegawa, M. Ishida, T. Nakajima, Y. Honda, O. Kitao, H. Nakai, M. Klene, X. Li, J.E. Knox, H.P. Hratchian, J.B. Cross, V. Bakken, C. Adamo, J. Jaramillo, R. Gomperts, R.E. Stratmann, O. Yazyev, A.J. Austin, R. Cammi, C. Pomelli, J.W. Ochterski, P.Y. Ayala, K. Morokuma, G.A. Voth, P. Salvador, J.J. Dannenberg, V.G. Zakrzewski, S. Dapprich, A.D. Daniels, M.C. Strain, O. Farkas, D.K. Malick, A.D. Rabuck, K. Raghavachari, J.B. Foresman, J.V. Ortiz, Q. Cui, A.G. Baboul, J.W. Clifford, J. Cioslowski, B.B. Stefanov, G. Liu, A. Liashenko, P. Piskorz, I. Komaromi, R.L. Martin, D.J. Fox, T. Keith, M.A. Al-Laham, C.Y. Peng, A. Nanayakkara, M.A. Challacombe, P.M.W. Gill, B. Johnson, W. Chen, M.W. Wong, C. Gonzalez, J.A. Pople, GAUSSIAN 03, Revision C.02, Gaussian, Inc., Wallingford, CT, 2004.
- [26] P. Pulay, G. Fogarasi, F. Pang, J.E. Boggs, *J. Am. Chem. Soc.* 101 (1979) 2550.
- [27] J.M.L. Martin, C. Van Alsenoy, GAR2PED, University of Antwerp, 1995.
- [28] J. Kruszewski, T.M. Krygowski, *Tetrahedron Lett.* 36 (1972) 3839.
- [29] M.L. Tosato, *J. Chem. Soc., Perkin Trans. 2* (1979) 1371.
- [30] M.L. Tosato, *J. Chem. Soc., Perkin Trans. 2* (1984) 1593.
- [31] M.L. Tosato, L. Soccorsi, *J. Chem. Soc., Perkin Trans. 2* (1982) 1321.
- [32] R.J. Boyd, C. Kim, Z. Shi, N.W.S. Weinberg, *J. Am. Chem. Soc.* 115 (1993) 10147.